Journal of NeuroVirology, 15: 411–424, 2009

ISSN 1355-0284 print / 1538-2443 online
DOI: 10.3109/13550280903473452

informa
healthcare

A limited innate immune response is induced by a replication-defective herpes simplex virus vector following delivery to the murine central nervous system

Zane Zeier,[1] J Santiago Aguilar,[2] Cecilia M Lopez,[1] GB Devi-Rao,[2] Zachary L Watson,[1] Henry V Baker,[1] Edward K Wagner, and [2] David C Bloom[1]

[1]Departments of Molecular Genetics and Microbiology, University of Florida College of Medicine, Gainesville, Florida, USA; and [2]Department of Molecular Biology and Biochemistry, University of California, Irvine, California, USA

Herpes simplex virus type 1 (HSV-1)–based vectors readily transduce neurons and have a large payload capacity, making them particularly amenable to gene therapy applications within the central nervous system (CNS). Because aspects of the host responses to HSV-1 vectors in the CNS are largely unknown, we compared the host response of a nonreplicating HSV-1 vector to that of a replication-competent HSV-1 virus using microarray analysis. In parallel, HSV-1 gene expression was tracked using HSV-specific oligonucleotide-based arrays in order to correlate viral gene expression with observed changes in host response. Microarray analysis was performed following stereotactic injection into the right hippocampal formation of mice with either a replication-competent HSV-1 or a nonreplicating recombinant of HSV-1, lacking the ICP4 gene (ICP4−). Genes that demonstrated a significant change ($P < .001$) in expression in response to the replicating HSV-1 outnumbered those that changed in response to mock or nonreplicating vector by approximately 3-fold. Pathway analysis revealed that both the replicating and nonreplicating vectors induced robust antigen presentation but only mild interferon, chemokine, and cytokine signaling responses. The ICP4− vector was restricted in several of the Toll-like receptor-signaling pathways, indicating reduced stimulation of the innate immune response. These array analyses suggest that although the nonreplicating vector induces detectable activation of immune response pathways, the number and magnitude of the induced response is dramatically restricted compared to the replicating vector, and with the exception of antigen presentation, host gene expression induced by the nonreplicating vector largely resembles mock infection. *Journal of NeuroVirology* (2009) **15**, 411–424.

Keywords: gene therapy; host response; HSV; vector

Address correspondence to David C. Bloom, Department of Molecular Genetics and Microbiology, Box 100266, University of Florida College of Medicine, Gainesville, FL 32610-0266, USA. E-mail: dbloom@ufl.edu

Received 29 April 2009; revised 2 September 2009; accepted 28 September 2009.

Introduction

Herpes simplex virus type 1 (HSV-1) is an enveloped icosahedral virus with a large (150-kb) double-stranded DNA genome. Normally, HSV-1 infects the oral mucosal epithelium and following primary infection, travels along sensory neurons to the trigeminal ganglion where it maintains a latent life cycle (Fields *et al*, 2001; Wagner and Bloom, 1997). During latency, only the non–protein-encoding latency-associated transcript (LAT) is produced from the otherwise inactive, nuclear, episomal viral genome. During reactivation from latency, virions retrace their path to the mucosal epithelium and reestablish lytic replication. Because HSV-1 only exhibits clinical reactivation and causes encephalitis in a subpopulation of hosts, it is apparent that unknown individual host differences play a crucial role in determining its pathogenesis. Therefore, characterization of these individual differences and the host response in general is of significant clinical importance.

HSV-1 has also been utilized for construction of recombinant viral gene therapy vectors (Burton *et al*. 2002). The large payload capacity, neural-transduction capability, and ease of construction make HSV-1 vectors amenable to applications within the central nervous system (CNS). Both nonreplicating HSV-1 vectors and antitumor replication-conditional HSV-1 vectors have great potential as therapeutic agents, but concerns regarding their toxicity and efficacy exist. Therefore, it is of interest to characterize the host response to HSV-1 vectors in the CNS for prevention of pathological consequences and for improving vector technology.

Viral infections of the CNS are unique because adaptive immunity is poorly induced. This is a result of the blood-brain barrier (BBB), lack of classic lymph drainage, and typical professional antigen-presenting cells (Lowenstein, 2002). Therefore, the most critical aspect of warding off HSV-1 in the CNS is the innate immune response, and, in particular, the interferon response (Mossman, 2005; Pasieka *et al*. 2006). Interferons (IFNs) can limit viral infection by regulating gene expression and modulating the subsequent immune response to infection; however, IFNs also contribute to the inflammatory response, which can be harmful to the host, and with regard to viral vectors, may limit transgene expression. Therefore, reducing IFN signaling and subsequent induction of innate immunity by attenuating HSV-1 vectors is essential to improving their efficacy.

Attenuation of HSV-1 for use as a vector can be achieved by mutating viral immediate-early (IE) genes such as ICP4 (DeLuca *et al*. 1985; Johnson *et al*. 1992, 1994). Previous analyses of host responses to differentially attenuated HSV-1 vectors *in vivo* have produced conflicting results. Some suggest that significant host responses are mounted, including inflammation and necrosis (Ho *et al*. 1995; Wood *et al*. 1994), yet others suggest minimal viral toxicity (Bloom *et al*. 1994; Burton *et al*. 2002; Dobson *et al*. 1990). In support of the latter, it was shown that neurophysiology was not altered in response to a highly attenuated vector (Bowers *et al*. 2003; Dumas *et al*. 1999; Olschowka *et al*. 2003). These seemingly contradictory findings are difficult to reconcile due to the diversity of vectors and analysis methods employed.

The goal of the current study was to characterize and compare the host response to an ICP4− HSV-1 viral vector to that of a replicating HSV-1 vector or vehicle (mock) following administration to the murine CNS. The replication-competent virus (HSVlacZgC) contained a *lacZ* reporter gene inserted into the nonessential viral glycoprotein C (gC) gene, and the replication-defective ICP4− vector (8117/43) contained the *lacZ* reporter inserted into the essential IE gene ICP4 (Dobson *et al*. 1990; Singh and Wagner, 1995). We chose the hippocampal formation as the site to inject the viruses. This region is a common target for gene therapy because this is an important center of learning and memory in the CNS. The hippocampus is also easy to anatomically identify and dissect. Viruses containing the *lacZ* reporter were selected to establish and verify stereotactic injection parameters that yielded consistent delivery of virus to the same anatomic region of the CNS. At 2 and 3 days following injection, the host response to these viruses was analyzed using Affymetrix microarrays in conjunction with cellular pathway analysis to provide a more comprehensive understanding of CNS responses to both HSV constructs. In addition, we employed an HSV-specific oligonucleotide–based spotted array to track viral gene expression (Aguilar *et al*. 2005). To our knowledge this is the first *in vivo* analysis of both host and viral gene expression during lytic and nonproductive HSV-1 infection following delivery directly to the CNS.

Results

Viral dissemination in the CNS following stereotactic injection

Both the HSVlacZgC and 8117/43 vectors contain *lacZ* reporter genes, allowing for visualization of viral gene expression by x-gal staining. Following stereotactic inoculation into the hippocampus as outlined in Figure 1, 8117/43 lacZ expression was mostly limited to the immediate area around the injection site in the CA1 region of the hippocampus, with some expression occurring in cortical neurons (Figure 2). Given the efficiency of HSV-1 axonal transport, it is not surprising that attenuated virus was found at distal locations. However, 8117/43 showed only modest changes in the expression pattern between the 2- and 3-day time points, consistent

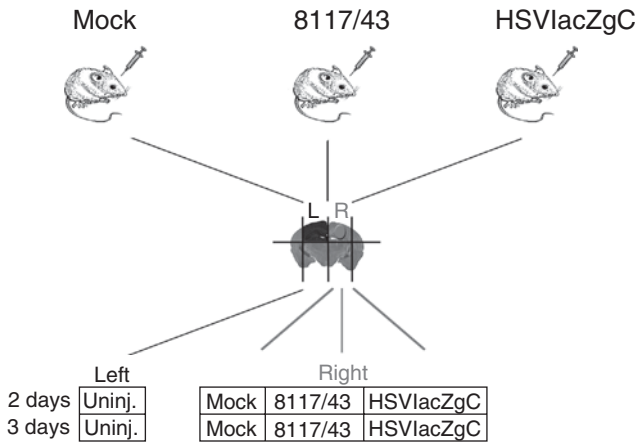

Figure 1. Experimental design of vector injections into the mouse CNS for microarray analysis. Vehicle (mock), 8117/43 (ICP4−), or HSVlacZgC (gC−) was injected into the right hippocampus of mice ($N = 9$). Tissue was collected from the injection site and from the contralateral (uninjected) side of mice at 2 and 3 days. For each experimental group, triplicate RNA samples, each pooled from three animals were analyzed by Affymetrix and HSV-specific microarrays.

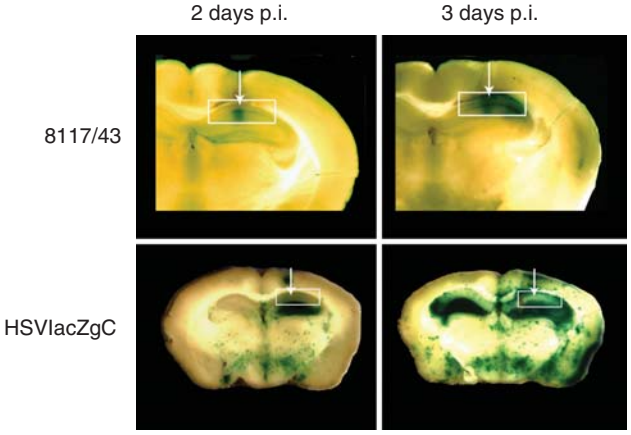

Figure 2. Coronal sections of mouse brains fixed and x-gal–stained 2 or 3 days following injection of either HSVlacZgC (gC−) or 8117/43 (ICP4−) HSV-1 viruses into the right CA1 region (*boxes*) of the hippocampus. Arrows indicate approximate injection track.

with its inability to replicate. In contrast, replication-competent HSVlacZgC demonstrated extensive *lacZ* expression that was not limited to the injection site (Figure 2), and x-gal staining revealed viral dissemination to the contralateral hemisphere at 3 days post infection (p.i). Viral gene expression analyses were performed at the peak of infection for the replicating virus.

Viral gene expression

An oligonucleotide-based, HSV-specific spotted array analysis of viral gene expression from tissue encompassing the HSVlacZgC injection site demonstrated a typical profile of viral gene expression of all kinetic classes at 3 days p.i. (Figure 3A) (Aguilar *et al*. 2005; Wagner, 2006; Stingley *et al*. 2000). Conversely, 8117/43 gene expression was very limited except for the latency associated transcript (Figure 3B). Although previous studies *in vitro* suggest that ICP4 mutants overexpress other IE genes in the absence of ICP4, our *in vivo* analysis did not corroborate that finding (Johnson *et al*. 1992, 1994). Overall, a comparison of the gene expression patterns of these two viruses in the hippocampus indicates that in contrast to the expected abundant lytic gene expression pattern exhibited by the replication-competent virus, the nonreplicating vector displayed an extremely restricted pattern of expression except for the LAT. We next wished to determine the effect of these two dramatically distinct viruses on the host gene expression using a mouse microarray.

Host gene expression

To compare the immunogenicity and cytotoxicity of the nonreplicating HSV-1 vector 8117/43 to those of a productive HSV-1 infection in the CNS, we analyzed gene expression using a mouse-specific microarray. Gene expression alterations induced by these viruses were compared to alterations induced by a mock infection (virus diluent) and to one another.

Apparent gene expression differences in mock-, 8117/43-, and HSVlacZgC-infected animals were identified at a significance threshold of $P < .001$. Probe sets and their expression in the biological replicates are visually represented after hierarchical cluster analysis as shown in Figure 4. Arrays from the HSVlacZgC infections at the 2- and 3-day time points clustered tightly together, whereas mock and 8117/43 arrays clustered in a separate node. This finding indicated that the mock and 8117/43 groups were more similar to one another than either is to HSVlacZgC, suggesting that the host response to an ICP4− HSV-1 vector is much more similar to mock injection than to a replication-competent virus. Furthermore, the figure shows that whereas there are clear gene expression differences as a result of HSVlacZgC infection, we were unable to delineate clear differences as a function of time after infection of the animals.

Mock versus 8117/43 analysis

To examine the host responses to mock injection and 8117/43, arrays from samples in each group were compared to arrays from the contralateral uninjected side of mock-injected animals. Because we did not observe large differences between the time points for the mock and 8117/43 groups, we combined and stratified the data set into mock- and 8117/43-treated categories.

Two groups of significant probe sets were identified (mock versus uninjected and 8117/43 versus uninjected) and separated into three groups: significantly altered probe sets specific to mock injection, probe sets common to both mock and 8117/43, and probe sets specific to 8117/43. From these analyses, 566 probe sets were found to be significantly

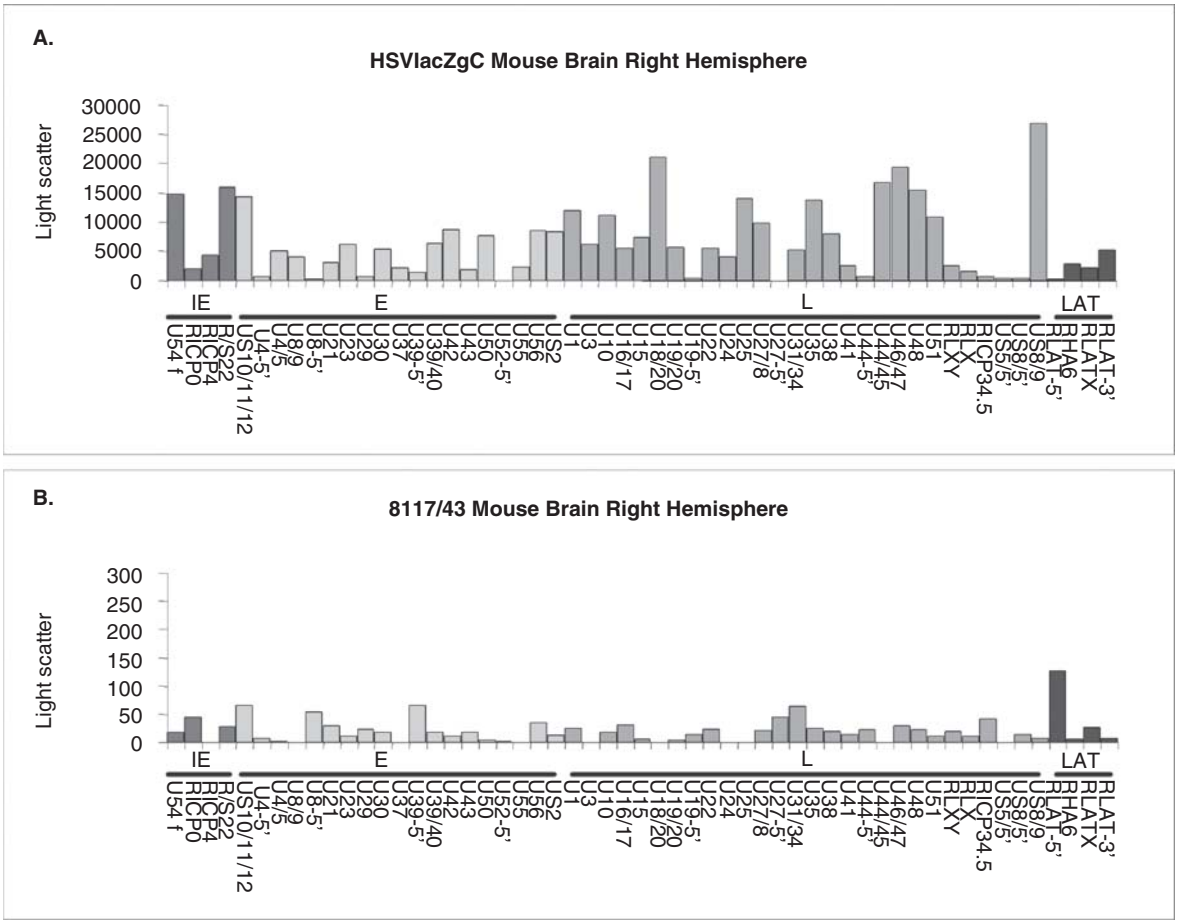

Figure 3. Immediate-early (IE), early (E), late (L), and latency-associated transcripts (LAT) HSV-1 viral gene expression as assayed by HSV-1–specific spotted arrays. Median resonance light scatter signal from triplicates representing viral gene expression 3 days p.i. of CNS tissue injected with (**A**) replication-competent HSVlacZgC (gC–) or (**B**) nonreplicating virus 8117/43 (ICP4–) 3 days p.i.

changed in the 8117/43 versus uninjected arrays and 405 in mock versus uninfected; with 226 common in both treatments. Of the 340 specific to 8117/43 injection ($P < .001$), 284 probe sets were up-regulated and 56 down-regulated. One hundred sixty of the up-regulated probe sets exceeded a 3-fold change. Mock injection induced 179 specific probe sets, 174 of which were up-regulated, with 19 probe sets exceeding a 3-fold change. Of the 226 significant probe sets common to both mock and 8117/43, almost all (225) were up-regulated, 40 of which exceeded a 3-fold change (Table 1). Groupings of probe sets were then analyzed using Ingenuity pathway analysis (IPA) (Calvano *et al*. 2005).

The 340 probe sets specific to 8117/43 were analyzed by IPA, which revealed that the host response to 8117/43 was dominated by the immune response, with nearly half (81 of 161) of the significant probe sets recognized by IPA falling into that category (Figure 5A). The most significant canonical pathway driving the immune response to 8117/43 was the antigen presentation pathway. Little induction of Toll-like receptor (TLR) signaling, interferon (IFN), and chemokine (CC) signaling was seen (Figure 5B). Furthermore, limited leukocyte extravasation signaling indicates a small inflammatory response to the nonreplicating vector. Two high-scoring molecular networks were generated by IPA and merged. Major nodes of this composite network include proinflammatory interleukin-6 (IL6), transcription factors STAT1 and STAT3, MYD88 (myeloid primary differentiation gene 88), and chemokine ligand 5 (CCL5 or RANTES). Other genes in the network include chemokine ligands, interferon factors (IRFs), and major histocompatability genes. A few of the most dramatically altered genes in this analysis include the interferon inducible protein 78 (MX1), which was up-regulated 80-fold. Others include complement factor β1 (CFB) up-regulated 107-fold, and IFIT1L, an interferon-induced protein, up-regulated 344-fold.

Only one high-scoring network was identified by IPA in an analysis of the mock-specific genes, its associated functions included cell growth, proliferation, and movement. Major nodes (genes with the most links to other genes in the network) include

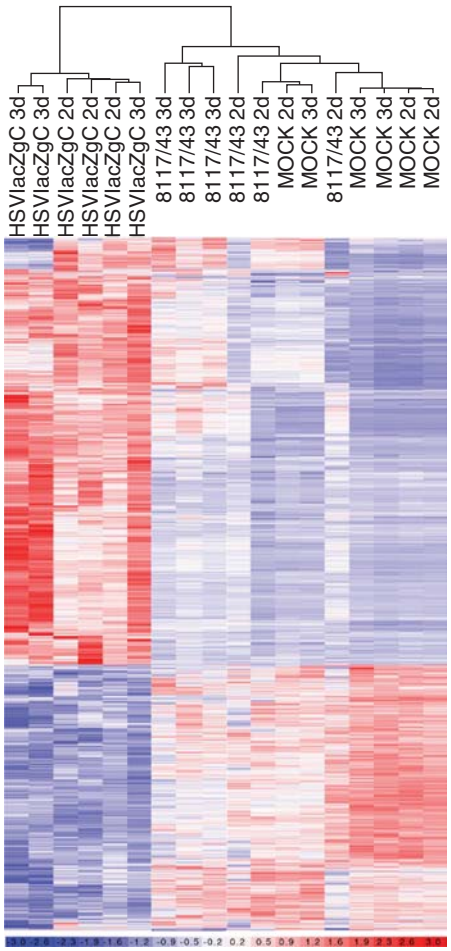

Figure 4. Supervised cluster analysis. HSVlacZgC (gC−)-, 8117/43 (ICP4−)-, and mock-injected arrays at 2 days (2d) or 3 days (3d) post injection. Red indicates up-regulation and blue indicates down-regulation of gene expression represented by fold-change.

cyclinD1 (CCND1) and integrin β1 (ITGB1) (data not shown).

To examine what biological functions are induced by both mock and 8117/43, the two highest-scoring networks constructed by IPA from the genes significantly altered by both 8117/43 and mock injection were combined (data not shown). The major biological function is the immune response (82 genes), and the major pathway is antigen presentation, with 7 of the 40 pathway genes significantly altered.

Table 1 Probe sets significantly altered by mock, 8117/43, or both were analyzed separately using IPA

	Mock vs. uninjected	Common	8117/43 vs. uninjected
Significant probe sets	179	226	340
Up-regulated	174	225	284
Down-regulated	5	1	56
>3-Fold Change	19	40	160
IPA recognized genes	104	140	161

Chemokine ligand 10 (CXCL10) and chemokine ligand 2 (CCL2) were up-regulated 243- and 40-fold by 8117/43, respectively, whereas the interferon-activated gene 202B was up-regulated 200-fold. Major network nodes include the transcription factor STAT3, TGFβ1 (transforming growth factor, beta 1), and ICAM (intracellular adhesion molecule 1).

8117 /43 versus HSVlacZgC

Because 8117/43 is replication-defective and extremely restricted in gene expression, it is likely that many of the alterations identified in the above analyses are due to responses initiated by virion proteins and limited IE expression. We next wished to examine how the changes induced by 8117/43 compared with a replication-competent HSV-1 virus HSVlacZgC. Arrays from 8117/43-injected samples were compared to arrays from HSVlacZgC-injected samples with mock-injected samples serving as a reference point (Table 2). Based on leave-one-out cross-validation and cluster analysis (data not shown), one of the 8117/43 specimens (081404A_81-2d-R) appeared to be an outlier and was removed from the data set before further analysis. At the 2-day time point, 206 probe sets were subsequently identified using the remaining arrays. At the 3-day time point, 253 probe sets were significantly altered ($P < .001$) by 8117/43. No arrays failed cross-validation of HSVlacZgC versus mock specimens.

To illustrate the total number of probe sets that were significantly altered by 8117/43 and HSVlacZgC infections, we pooled the probe sets from both postinfection time points, counting a probe set only once if it was altered at both times. Roughly 3 times more probe sets were altered in response to HSVlacZgC than in response to 8117/43, with only 256 probe sets that were altered by both constructs. In both cases most probe sets significant at $P < .001$ were altered more than 3-fold, and most were up-regulated (Table 2).

Both 8117/43 and HSVlacZgC induced alterations in genes associated with the immune response (Figure 6A). In the case of 8117/43, 59 immune response genes were altered at 3 days, whereas 239 genes were altered by HSVlacZgC at the same time point. Immune and lymphatic system development and function were more significantly represented in the HSVlacZgC comparison, as was cell movement and cell death. Induction of the viral infection category was similar in both 8117/43 and HSVlacZgC comparisons, with surprisingly little up-regulation.

Because HSVlacZgC altered the expression of many more genes than 8117/43, one might expect more genes to be assigned to a given pathway simply by chance. To account for such an issue, IPA calculates the probability, or significance, that a given pathway is assigned to the data set by chance rather than calculating the ratio of genes in a pathway from

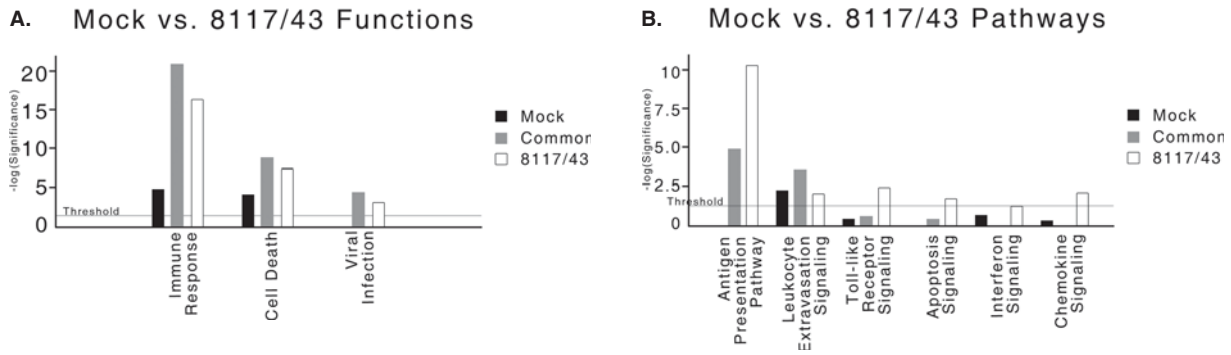

Figure 5. IPA of genes altered by mock, 8117/43, or genes altered by both mock and 8117/43 versus uninjected samples. (**A**) Selected biological functions and (**B**) canonical pathways. The *y*-axis (−log of the *P* value) is the probability that each biological function was assigned to the gene set by chance alone. Threshold is indicated by a line and corresponds to $P < .05$. Analysis and figure generation were performed using IPA with permission (Ingenuity® Systems, www.ingenuity.com).

the data set to the total number of genes in a pathway. Based on this measure of significance, 8117/43 strongly induced the antigen presentation pathway and, to a lesser extent, interferon and chemokine signaling (Figure 6B). Although both 8117/43 and HSVlacZgC induced gene expression changes in about the same number of genes in the antigen presentation pathway, induction by 8117/43 was more significant. Antigen presentation pathway genes that were up-regulated by 8117/43 included three major histocompatability class I genes (HLAC, HLAE, HLAF), three major histocompatability class II genes (HLADQB2, HLADQA1, HLADMB), two proteolytic antigen processing peptidase genes (PSMB8, PSMB9), both tap1 and tap2 transporter genes, as well as the tap binding protein (TAPBP). At the 2-day time point, 8117/43 up-regulated 4 out of 19 genes in the IFN pathway (IFNb1, ISGF3G [ISG9], STAT1, and STAT2). HSVlacZgC did not significantly induce IFN signaling; however, it induced STAT1 and STAT2 similar to 8117/43. Although chemokine ligands CCL2 (MCP-1), CCL5 (RANTES), and CCL7 (MCP-3) were up-regulated at both 2- and 3-day time points for 8117/43 and HSVlacZgC injections, fold-change values tended to be much higher for HSVlacZgC than for 8117/43, likely reflecting a more robust induction as a result of viral replication. In addition, other chemokine pathway molecules were induced by HSVlacZgC, including CCL4, CCL11, CCL13, as well as c-Fos and c-Jun transcription factors. HSVlacZgC strongly up-regulated Toll-like receptor (TLR) signaling, leukocyte extravasation, nuclear factor kappa B (NFκB), and death receptor and apoptotic signaling pathways. The death receptor and apoptotic signaling pathways have many genes in common, and in our analysis the same genes were found in both pathways for HSVlacZgC, including caspases 7, 8, 12, and tumor necrosis factor (TNF). Daxx was up-regulated by both viruses, but 8117/43 did not significantly induce either pathway at 2 days or 3 days. Double-stranded RNA-dependent protein kinase (PKR) (EIF2AK2) and TLR3 were up-regulated at both time points, and for both viruses, but HSVlacZgC induced additional TLR signaling genes, including MYD88, TLRs 2, 4, 6, 7, and Map3k1 (MAPK).

IPA identified one high-scoring network at 2 days for 8117/43. Major nodes included IRF1 and STAT1. At 3 days p.i., one high-scoring network was identified, also having STAT1 and IRF1, but also IRF7, TNFSF10, and IFB1 as major nodes. In addition, many networks were identified by IPA in the HSVlacZgC conditions at both 2 and 3 days p.i.; four of them were merged. Major nodes of the merged networks included IL6, TGFβ1, and TNF (data not shown).

Table 2 Probe sets significantly altered by 8117/43 and HSVlacZgC

	8117/43 vs. mock		HSVlacZgC vs. mock	
	2 days* p.i.	3 days p.i.	2 days p.i.	3 days p.i.
Total probe sets	206	253	930	1204
>3-Fold change	180	184	479	716
Up-regulated	197	229	681	1014
Down-regulated	9	24	249	190
IPA recognized genes	103	117	399	545

*The 812-day outlier array was removed.

Reverse transcriptase–polymerase chain reaction (RT-PCR) validation of microarray data

The wide net cast by microarray experiments allows for a genome-wide view of gene expression changes after exposure to a pathogen. In contrast, quantitative real-time RT-PCR allows for pinpointing measurement of specific gene activation or repression. To complement the information gleaned from microarray analysis of intracranial injections with HSV, we chose 12 genes critical to one or more viral host-response pathways for specific expression analyses: Casp8 and Daxx (apoptosis), Ccl5 (chemokine signaling), Cfb (complement), Eif2ak2 (protein synthesis), Il6 (interleukins), Irf7 (interferon response), Mx2

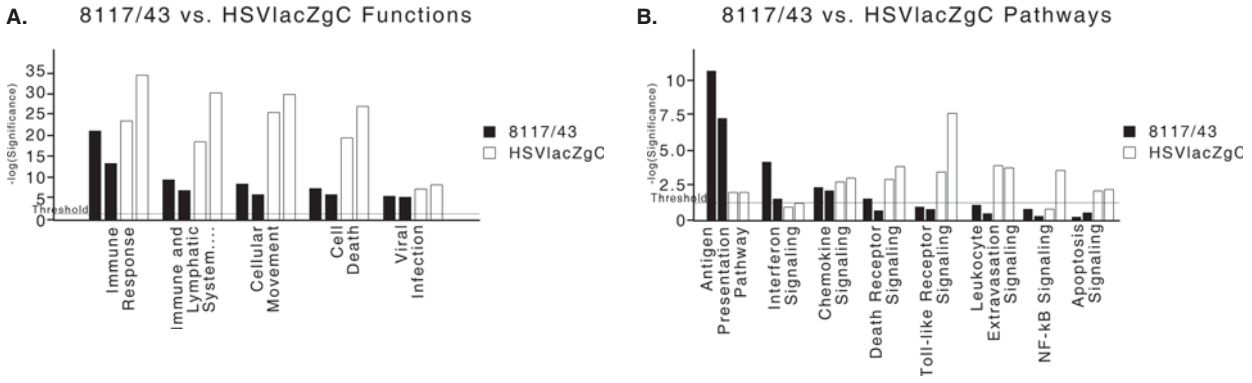

Figure 6. Biological functions induced by 8117/43 and HSVlacZgC. (**A**) Selected biological functions and (**B**) canonical pathways induced by 8117/43 and HSVlacZgC at 2 days (first and third bars in each pathway) and 3 days (second and fourth bars) are shown. Analysis and figure generation were performed using Ingenuity Pathway Analysis with permission (Ingenuity Systems).

(virus resistance), Psmb9 (proteasomal antigen processing), Tap1 (MHC class I antigen presentation), and Tlr2 and Tlr3 (Toll-like receptors). Microarray analysis revealed that all were significantly up-regulated in HSVLacZgC-injected mice relative to mock-injected animals at 3 days post injection, whereas all except for Casp8 and Il6 were significantly up-regulated in 8117/43-injected mice at the same time point ($P < .001$; Table 3). Real-time RT-PCR analysis of the selected gene products indicated that all selected mRNAs were up-regulated in HSVLacZgC-injected mice relative to mock, whereas all except Il6 were up-regulated in 811743-injected mice relative to mock ($P < .05$) (Table 3). The only exception was Casp8, which was found by RT-PCR but not by microarray to be significantly up-regulated in 8117/43-injected mice relative to mock. However, it is worth noting that the fold-increase of Casp8 mRNA expression was determined to be rather modest in both cases (1.5-fold by microarray, 2.8-fold by RT-PCR). Overall, the strong concordance between data sets serves to validate the mRNA expression values as determined by microarray.

Immunohistochemical detection of Cd11b/c immunocytes

In the CNS microglia represent an abundant form of brain macrophages (Guillemin and Brew, 2004). They are primary mediators of antigen presentation and contribute to inflammatory signaling. Resting (ramified) microglia have a branched morphology that transforms to a small rod shape when activated in response to injury. This activation is at a

Table 3 Validation of microarray data by quantitative real-time RT-PCR

	Fold increase relative to mock[a]			
	811743		HSVLacZgC	
Gene product (designation)	Microarray	RT-PCR	Microarray	RT-PCR
Caspase 8 (Casp8)	1.5	2.8**	6.3*	4.4**
Chemokine, C-C motif, ligand 5 (Ccl5)	10.1*	30.4**	45.1*	34.0**
Complement factor B (Cfb)	15.9*	19.1**	80.5*	23.2**
Fas death domain associated protein (Daxx)	2.1*	3.0**	7.5*	3.8**
Eukaryotic translation initiation factor 2 alpha kinase 2 (Eif2ak2)	4.5*	7.1**	5.8*	5.6**
Interleukin 6 (Il6)	1.2	2.9	111.4*	26.8**
Interferon regulatory factor 7 (Irf7)	25.1*	15.8**	50.2*	15.1**
Myxovirus resistance 2 (Mx2)	16.2*	11.6**	52.8*	10.4**
Proteasome subunit, beta type 9 (Psmb9)	11.8*	13.3**	24.3*	8.3**
Transporter 1, ATP-binding cassette (Tap1)	13.3*	9.7**	30.5*	9.4**
Toll-like receptor 2 (Tlr2)	1.7*	3.7**	9.8*	5.5**
Toll-like receptor 3 (Tlr3)	2.8*	3.4**	5.0*	2.7**

[a]Comparison of increases in mRNA expression levels of 12 selected gene products between 811743- or HSVLacZgC-injected mice relative to mock-injected at 3 days post injection as determined by microarray and real-time RT-PCR.*mRNA expression, as determined by microarray, is significantly increased relative to mock ($P = .001$).**mRNA expression, as determined by RT-PCR, is significantly increased relative to mock ($P = .05$).

maximum approximately 2 to 3 days following an injurious event, corresponding with the time points of the microarray analysis in the present study.

We wished to verify the microarray analysis by examining the level of activation of microglia and other brain macrophages, since microarray analysis indicated robust immune gene expression, including inflammation and antigen presentation pathways to HSVlacZgC and 8117/43. Coronal sections of mouse brains were stained with a Cd11b/c reactive antibody. The commonality of these markers among brain macrophages, including microglia, pericytes, and perivascular macrophages, as well as the similarity in cellular morphology among activated forms of these cells, precludes specific classification of positively stained cells (Guillemin and Brew, 2004). Furthermore, the disruption of the blood-brain barrier (BBB) likely allows for infiltration of blood-borne monocytes and macrophages that are not easily distinguished from reactive microglia (Banati, 2003). Nevertheless, an obvious distinction between the experimental groups can be made with respect to the number of brain macrophages located near the site of injection, as well as the level of cytopathology. Specifically, both parameters increased in response to both HSVlacZgC (Figure 7A) and 8117/43 (Figure 7B), but were most pronounced in HSVlacZgC-injected brains. Little staining was seen in tissue from mock-injected animals (Figure 7C). However, at a higher concentration of primary antibody, steady-state levels of ramified microglia could be readily observed (data not shown). Only a few reactive microglia were observed in mock-injected tissue, and only near the site of injection.

These observations corroborate our microarray analysis, as they indicate a more robust immune response to HSVlacZgC than to 8117/43. Furthermore, the infiltration and proliferation of these cells near the site of injection implicate them as a source of increased antigen presentation and inflammatory gene expression that was observed in the microarray analysis.

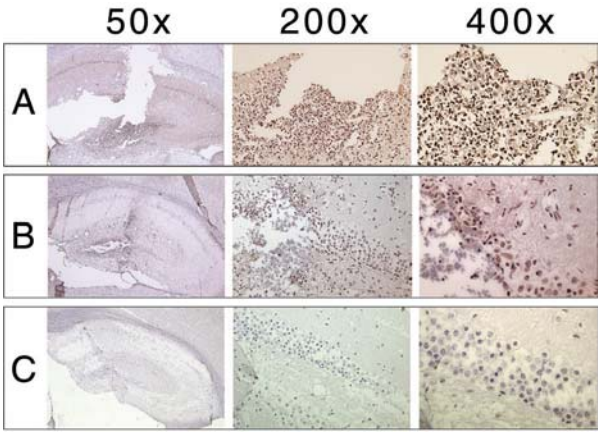

Figure 7. Immunohistochemical visualization of Cd11b/c-positive brain macrophages. Three days following (**A**) HSVlacZgC, (**B**) 8117/43, or (**C**) mock injections, animals were perfused, tissue collected, stained with a polyclonal antibody against Cd11b/c (*brown*), and counterstained with hematoxalin (*blue*).

Discussion

Several aspects of neuroimmunology make HSV-1 infections of the CNS unique (Lowenstein, 2002; Peterson and Remington, 2000; Wagner, 2006). First, the CNS lacks classical lymph drainage and professional antigen-presenting cells, limiting priming of adaptive immunity. Secondly, valuable neurons are somewhat protected from cytolytic T-lymphocyte (CTL) activity, and rather than eliminating them, CD8+ and CD4+ cells contribute by producing IFN-γ to aid infected neurons by setting up an antiviral state. Third, the selective permeability of the BBB isolates the CNS to an extent (although it is easily disrupted) from molecules such as cytokines and immunoglobulins, as well as limits access to immunocytes. Infiltration of leukocytes such as natural killer (NK) cells and macrophage/monocytes occurs, but neutrophils are less efficiently attracted due to low levels of P-selectin on the BBB endothelium (Peterson and Remington, 2000). These factors indicate that innate immunity plays a critical role in warding off HSV-1 infection in the CNS, which can limit long-term transgene expression from nonreplicating vectors. In the present work, we have determined the degree to which innate immunity is induced by HSV-1 *in vivo* and to what extent non–replication-competent vectors induce innate immunity. Additionally, we have established what other host-response mechanisms are induced by these vectors.

Microarray technology has been employed by other groups to examine the host response during latency and in response to reactivation stimuli (Higaki *et al*. 2002; Hill *et al*. 2001; Kramer *et al*. 2003; Tsavachidou *et al*. 2001), whereas others have examined the cellular response during lytic infections *in vitro* (Brukman and Enquist, 2006; Eidson *et al*. 2002; Khodarev *et al*. 1999; Pasieka *et al*. 2006; Taddeo *et al*. 2002). Despite the advantages of microarray analysis, some shortcomings limit its utility. Because microarray analysis only reveals the steady-state level of a given transcript and cannot reveal the rate of mRNA synthesis or degradation, it represents a snapshot of a dynamic process. This consideration becomes especially important in viral studies because some viral genes can induce a generalized reduction in mRNA not specific to any biological process. For example, the HSV-1 viral host shut-off (VHS) protein nonselectively degrades mRNA, whereas ICPO can alter transcription by modulating RNA pol II and disrupting ND10 structures. HSV-1 is also notorious for redirecting cellular

protein functions and is capable of altering cell biology at the level of proteins, a process that cannot be directly traced by array analysis. Also, microarray analysis is not likely to discriminate between pre-mRNA and spliced mRNA, an important aspect when one considers ICP27's ability to inhibit splicing. Another consideration in using microarray analysis for *in vivo* studies is that not only do these studies examine a population of cell types, including infiltrating cells, which can add variability to the microarray analysis, but also the stage of viral infection is varied across the tissue sample and is not able to be synchronized as with *in vitro* studies. Despite these limitations, we have characterized the host response to both replication-competent and nonreplicating HSV-1 when delivered directly to the CNS and have identified specific aspects of the innate response that seem to be dominant in HSV-1 infections.

The interferon response

In our analysis, very little IFN induction was seen in response to a mock injection or 8117/43 when the two were compared to arrays from uninjected samples. Neither group met the significant threshold of IFN induction in IPA analysis, although several gene members of the pathway were differentially expressed. When 8117/43 and HSVlacZgC were compared to mock arrays at separate time points, 8117/43 did reach threshold significance in IPA, whereas HSVlacZgC did not. Therefore, 8117/43 does alter the expression of some gene members of the IFN pathway, but whether this represents a significant induction in an IPA analysis is dependent upon the broader context of the analysis.

Others have suggested that ICP4 mutants do not strongly induce an IFN response *in vitro*, perhaps due to ICP0 activity (Eidson *et al*. 2002; Lin *et al*. 2004; Mossman, 2005), whereas others claim that γ34.5 is critical (Pasieka *et al*. 2006). Our analysis demonstrates that HSVlacZgC, having both ICP0 and γ34.5 at its disposal, did not induce a strong IFN response; it is formally possible that the lack of IFN induction by HSVlacZgC is partially due to the gC mutation, though the fact that gC mutants are only minimally attenuated in virulence and spread *in vivo* argues against the gC mutation playing a major role (Friedman *et al*. 1996). In contrast, 8117/43 did seem to induce changes in expression of some (4 of 19) IFN pathway molecules, including STAT1 and STAT2, as well as IFNb1 and ISG9. We conclude that 8117/43 induces a mild IFN response and that this response may be only partially blocked by its low level of ICP0 expression.

Toll-like receptor signaling

Toll-like receptors (TLRs) are an innate immune host-defense mechanism that detects common microbial peptide and nucleotide patterns. TLRs 2 and 9 likely recognize HSV-1 glycoprotein D, and TLR3 detects double-stranded RNA (dsRNA) common to viral transcriptomes. TLRs signal through NFκB to induce type I IFNs, as well as chemokines and cytokines, which lead to inflammation and recruitment of lymphocytes (Morrison, 2004). However, TLR signaling may not completely protect the host against HSV-1 signaling, since TLR2−/− mice actually had less inflammation and less mortality during HSV-1 infections (Kurt-Jones *et al*. 2004). Our results demonstrate a strong induction of TLR signaling pathways for HSVlacZgC but not 8117/43, although both viruses induced PKR and TLR3.

Antigen presentation

The most striking finding of our study is the robust induction of antigen presentation in response to both 8117/43 and HSVlacZgC. Both viruses induce genes involved with multiple stages of antigen processing, including proteolytic degradation, transport, and major histocompatibility complex (MHC) I and MHC II presentation to CD8+ and CD4+ lymphocytes, respectively. In our analysis, it is impossible to determine exactly what cells are presenting antigen; however, it is likely that non-neuronal cells are the source of MHC I presentation, as neurons normally do not have MHC I or MHC II presentation. Resident antigen-presentting cells (APCs) of the CNS are likely the source of MHC II antigen presentation (Lowenstein, 2002; Peterson and Remington, 2000).

The lack of professional APCs, and lack of lymph drainage in the CNS, means that poor adaptive immune priming takes place regardless of antigen presentation (Lowenstein, 2002). If care is taken not to disrupt the tissue, then virus may be delivered without causing significant production of neutralizing antibody, as has been shown with adeno-associated virus (AAV) vectors (Peden *et al*. 2004). With respect to viral vectors, this is encouraging, as it allows for vector readministration strategies to be employed.

NFκB

Inhibition of NFκB reduces viral titers (Amici *et al*. 2001) and many genes associated with the NFκB pathway are induced by HSV-1, likely due to PKR activation (Taddeo *et al*. 2002, 2003) and may inhibit apoptosis mediated by TNF (Goodkin *et al*. 2003, 2004; Wagner, 2006). However, this is a point of contention, as others suggest that NFκB induction does not prevent apoptosis, because infection of NFκB–defective mice is not associated with increased apoptosis (Taddeo *et al*. 2004).

Our analysis shows a mild induction of NFκB by HSVlacZgC at 2 days and a strong induction of NFκB at 3 days p.i., but not by 8117/43 at either time point. This induction of NFκB by HSVlacZgC does not correlate with a reduction of apoptotic signaling over the same two time points, suggesting that NFκB may not preclude apoptosis.

Apoptosis
Several HSV-1 E and L genes (ICP6, γ34.5, and gD) are able to block apoptosis, which is mediated by caspases and induced by TNF and Fas signaling (Wagner, 2006). Our data show significant up-regulation of the related pathways of apoptotic and death receptor signaling in response to HSVlacZgC, but not to 8117/43. Only HSVlacZgC infection was associated with induction of apoptotic pathways despite its expression of antiapoptotic viral genes. We conclude that induction of apoptotic and death receptor pathways is much more robust in response to HSVlacZgC than to 8117/43 due to the replication competence of HSVlacZgC rather than antiapoptotic viral functions.

Chemokines
Proinflammatory chemokine signaling can be particularly harmful in a confined organ such as the brain and may not effectively limit HSV-1 infections (Marques *et al*. 2004, 2006). However, HSV-1 does not induce an immunopathogenic effect in mice as robustly as other alphaherpesviruses such as HSV-2 and pseudorabies virus (PRV) (Paulus *et al*. 2006).

In our analysis, we found more robust induction of chemokine receptor ligands, monocyte chemoattractant protein (MCP)-1, MCP-3, and RANTES following HSVlacZgC infection than following 8117/43 infection. Several other chemokine ligands were induced by HSVlacZgC, as well as the transcription factors c-Fos and c-Jun. Taken together, these data indicate a stronger chemokine-mediated inflammatory response to HSVlacZgC than to 8117/43, which only mildly induced chemokine signaling at 3 days when compared to mock injection.

Cytokines
IL6 and IL10 signaling were both significantly up-regulated by HSVlacZgC, but not by 8117/43, at the separate 2- and 3-day time points. TNF and TGF were both significantly up-regulated by HSVlacZgC and 8117/43. Although somewhat contradictory, it is obvious that the inflammatory response to HSVlacZgC was much greater than to 8117/43, which closely resembled mock infection.

In summary, our analyses demonstrate that with the exception of antigen presentation pathways, ICP4− HSV-1 vectors exhibit low levels of induction of most innate and inflammatory pathways following delivery to the CNS. An important caveat, however, is the fact that antigen presentation pathways remain similar to that of a replicating virus, though the recruitment and activation of microglia by the ICP4− vector are significantly reduced. The impact of this response on the development of localized and systemic acquired immunity to specific transgenes will probably need to be assessed on a case-by-case basis.

Materials and methods

Viruses
The replication-incompetent ICP4 deletion 8117/43 virus (Dobson *et al*. 1990) was obtained from J. Stevens and amplified on complementing E5 cells obtained from N. DeLuca (DeLuca *et al*. 1985) in Eagle minimum essential medium (MEM) with 10% fetal bovine serum, penicillin (100 U/ml), and streptomycin (100 μg/ml). Cells were maintained at 37°C under 5% carbon dioxide. The replication-competent virus HSVlacZgC (Singh and Wagner, 1995) contains a *lacZ* reporter gene driven by the promoter from the HSV-1 UL50 (dUTPase) gene (early gene kinetics) inserted into the nonessential viral glycoprotein C (gC) locus. HSVlacZgC was amplified on rabbit skin (RS) cells in MEM with 5% calf serum, penicillin (100 U/ml), and streptomycin (100 μg/ml). 8117/43 stock was titrated on 24-well plates of E5 cells; the final concentration was 6×10^8 plaque forming units (p.f.u.)/ml. HSVlacZgC was titrated on RS cells in similar fashion with a final concentration of 2.5×10^8 p.f.u./ml.

Stereotaxic injection
Female ND4 Swiss mice aged 6 to 8 weeks were obtained from Harlan Sprague-Dawley. Nine mice per experimental group were used. On the day of surgery, animals were anesthetized with ketamine (70–80 mg/kg)/xylazine (14–15 mg/kg), and an incision was made along the midline of the skull. A burr hole was made in the skull and a single 1-μl injection of 8117/43, HSVlacZgC, or vehicle (MEM with 10% fetal bovine serum [FBS]) was delivered via cannula into the right CA1 region of the hippocampal formation (AP = −0.19 cm, L = −0.15 cm, V = −0.17 cm) at a rate of 0.35 μl/min. Following injections, bone wax was used to repair the burr hole, and a surgical staple was used to close the wound.

Tissue collection
After 2 or 3 days, animals were anesthetized with halothane and euthanized by cervical dislocation. A 1-mm^3 tissue sample was immediately collected from the CA1 region of the hippocampus surrounding the injection site and from the same region of the contralateral, uninjected hippocampi of vehicle (mock)-injected mice. Both tissue samples were immediately placed in 5 volumes of RNA later (Figure 1).

X-gal staining
Two animals from each *lacZ* reporter virus-injected experimental group were prepared for x-gal staining by deep anesthesia with xylene (8 mg/kg), ketamine (24 mg/kg), and acepromazine (80 mg/kg), followed by perfusion with 4% paraformaldehyde. Brains were sectioned using a brain blocker and placed in

x-gal fixation solution (0.1% sodium deoxycholate [NaDOC], 0.02% NP-40, 2% formaldehyde, 0.2% glutaraldehyde, 0.1 M HEPES [pH 7.4], 0.875% NaCl) for 1 h at 4°C. Tissue samples were washed 2× in phosphate-buffered saline (PBS) and 1× in PBS/DMSO (3%) and incubated overnight at 31°C in x-gal staining solution (0.15 M NaCl, 100 mM HEPES [pH 7.4], 2 mM $MgCl_2$, 0.01% NaDOC, 0.02% NP-40, 5 mM potassium ferricyanide, 5 mM potassium ferrocyanide, 1 mg/ml x-gal [from a 20 mg x-gal/ml dimethylformamide stock]).

RNA preparation

Extraction of total RNA from brain-tissue samples (approximately 60 mg) was carried out using the RNeasy midi kit (Qiagen) according to the manufacturer's protocol, with some modification in homogenization. Approximately 30 μg of total RNA were typically obtained.

Microarray hybridization

Isolated total RNA samples were processed as recommended by Affymetrix (Affymetrix GeneChip Expression Analysis Technical Manual; Affymetrix, Santa Clara, CA) at the University of California, Irvine, DNA and Protein MicroArray Facility. In brief, total RNA samples were quality assessed using an Agilent Bioanalyzer 2100 (Agilent Technologies, Palo Alto, CA) and adjusted to a final concentration of 1.25 μg/μl. cDNA was synthesized from the total RNA (typically 10 μg total RNA starting material each sample reaction) using the SuperScript Double-Stranded cDNA Synthesis Kit (Invitrogen, Carlsbad, CA) and poly (T)-nucleotide primers. Biotin-tagged cRNA was then generated using the Affymetrix GeneChip IVT Labeling Kit. Subsequently, 10 μg of fragmented target cRNA was hybridized at 45°C for 16 h to probe sets present on an Affymetrix MOE430Av2 array. The GeneChip arrays were washed and then stained (streptavidin-phycoerythrin [SAPE]) on an Affymetrix Fluidics Station 450, followed by scanning on a GeneChip Scanner 3000 7G. The results were quantified and analyzed using GCOS 1.2 software (Affymetrix) using default values (Scaling, Target Signal Intensity = 500; Normalization, All Probe Sets; Parameters, all set at default values).

Data analysis

Affymetrix murine microarrays

Normalization and creation of a gene-expression matrix was performed using the perfect-match-only method by inputting data (.cel files) into dChip (Li and Wong, 2001). Probe sets with signal intensities below background levels on all arrays as calculated by an Affymetrix detection algorithm were removed from the analysis. Statistical algorithims implemented in BRB array tools (version 3.5.0-beta 1, developed by Richard Simon, Amy Peng Lam, Supriya Menezes, National Cancer Institute and EMMES) was used throughout this study.

Supervised analysis. Supervised analysis was conducted using genes that were identified as significant ($P < .001$) between the treatment groups as determined by an *F*-test. The ability of significant genes to distinguish between treatment groups was assessed by leave-one-out cross-validation studies. The ability of gene expression classifiers to correctly predict the class label of the array left out of the analysis was estimated using Monte Carlo simulations.

Unsupervised analysis. Probe sets that exhibited a hybridization signal intensity with a coefficient of variation of greater than 0.5 were identified and subjected to hierarchical cluster analysis using algorithms implemented in dChip.

Pathway analysis. The chief molecular functions and biological processes were analyzed by Ingenuity pathway analysis (IPA; Ingenuity Systems, Redwood City, CA). Fischer's exact test was used to calculate a *P* value.

HSV-1 spotted arrays

HSV-1 RNA was analyzed by the resonance light scattering (RLS) method as in previous publications (Aguilar *et al*. 2006; Sun *et al*. 2004). For each microarray, 10 μg of RNA was used to synthesize labeled cDNA using the HiLight dual-color kit (Invitrogen). HSV-1 oligonucleotide arrays were constructed as previously described (Wagner *et al*. 2002; Yang *et al*. 2002). Hybridizations were carried out in 5x SSC = 0.75M NaCl, 0.75M sodium citrate, 0.2% sodium dodecyl sulfate (SDS) at 52°C in a MAUI hybrid mixer assembly for 18 h. After hybridization the slides were processed as described in the labeling kit instructions. Microarrays were scanned with a GSD-501 HiLight reader (Invitrogen) and analysis of the signals was carried out as described previously (Sun *et al*. 2004).

Real-time RT-PCR analysis of cellular RNAs

For RNA isolation, mice were injected intracranially as described for the microarrays. At 3 days post injection, mice were sacrificed and tissue was harvested from the injection site and placed in RNAlater (Ambion). Tissue samples were homogenized in 1 ml 4 M guanidine thiocyanate (GTC) solution, pH 7.0 (4 M GTC, 0.017 M sodium *N*-lauroyl sarcosine, 0.025 M sodium citrate, 0.7% 2-mercaptoethanol, 0.1% Antifoam A), and processed as described (Chirgwin *et al*. 1979) with 0.1 ml of the homogenate retained for DNA analysis. To remove genomic contamination, RNA was treated with Turbo DNAfree (Ambion) according to the manufacturer's protocol.

For cDNA synthesis, 1 μg of each RNA sample was reverse transcribed using the Omniscript RT Kit (Qiagen) according to the manufacturer's protocol. RT reactions were performed in a total volume of 40 μl. "No-RT" reactions, containing 0.5 μg of RNA and diethylpyrocarbonate (DEPC) H_2O in a total volume of 20 μl, were performed to control for genomic DNA contamination. Samples were diluted 1:10 for use in real-time PCR.

Expression levels of target genes and the endogenous cellular control gene, *XIST*, were evaluated using TaqMan Gene Expression Assays (Applied Biosystems). Primer/probe sets consisted of two unlabeled PCR primers and the FAM dye–labeled TaqMan MGB probe in a single mixture. All probes were designed across an intron-exon junction to eliminate signal from potential genomic DNA contamination. The primer/probe sets used in this study were CASP8 (ABI Assay ID Mm00802247_m1); CCL5 (ABI Assay ID Mm01302428_m1); CFB (ABI Assay ID Mm00433909_m1); DAXX (ABI Assay ID Mm00492089_m1); EIF2AK2 (ABI Assay ID Mm00440966_m1); IL6 (ABI Assay ID Mm00446190_m1); IRF7 (ABI Assay ID Mm00516788_m1); MX2 (ABI Assay ID Mm00488995_m1); PSMB9 (ABI Assay ID Mm00479004_m1); TAP1 (ABI Assay ID Mm00443188_m1); TLR2 (ABI Assay ID Mm00442346_m1); TLR3 (ABI Assay ID Mm00446577_g1); and XIST (ABI Assay ID Mm01232884_m1).

Quantitative real-time PCR was performed using an ABI PRISM 7900HT Sequence Detection System (Applied Biosystems). All reactions were performed in triplicate reactions of a total volume of 20 μl each. Briefly, all reaction mixtures contained 3 μl of cDNA template, 10 μl of TaqMan Universal PCR Master Mix–No AmpErase UNG (2×; Applied Biosystems), 1 μl of the appropriate TaqMan Gene Expression Assay, and 6 μl of dH_2O. Thermal cycling conditions were as follows: one cycle at 50°C for 2 min followed by 95°C for 15 min, then 40 cycles of 95°C for 15 s and 60°C for 1 min. Threshold cycle (C_T) values were obtained using SDS 2.2.1 software and relative gene expression was calculated using the standard curve method. Each sample's experimental assay expression values were then normalized to its mean *XIST* gene assay expression value. Statistical analyses were performed using a two-sample *F*-test for homoscedasticity, followed by the appropriate Student *t* test for population means.

Immunohistochemistry

Three days following stereotaxic injection, animals were perfused with ice-cold 4% paraformaldehyde, and brains were removed and postfixed overnight. Subsequently, the tissue was transferred to 70% ethanol and paraffin embedded. Five-micron coronal sections were collected from the region of injection and deparaffinized in xylene. Endogenous peroxidase activity was blocked using a 3% hydrogen peroxide/97% methanol solution, and sections were then rehydrated and treated with proteinase K (Dako S3020) for 2.5 min to unmask epitopes. Endogenous avidin/biotin activity was blocked using a Vector Laboratories kit (SP2001). Following serum blocking (goat), a polyclonal rabbit anti-Cd11b/c primary antibody (Abcam ab53817) was then applied at a concentration of 2.5 μg/ml in Zymed solution overnight at 4°C. A secondary antibody solution was applied for 30 min at room temperature (5 μl biotinylated goat anti-rabbit antibody, 15 μl goat serum, in 1 ml Tris-buffered saline–Tween [TBS-T = 0.05M Tris; 0.150 NaCl, 0.1% Tween 20, pH 7.6]). Visualization of antibody binding was achieved using a Vector Laboratories ABC elite kit (PK-7200), and DAB substrate kit (SK-4100) and sections were counterstained with hematoxylin.

Acknowledgement

The authors thank N. Giordani for helpful comments on the manuscript.

Declaration of interest: This work was supported in part by NIH grants AI48633 (D.C.B.) and CA11861 (E.K.W.) as well as an Investigator in the Pathogenesis of Infectious Disease Award from the Burroughs Wellcome Fund (D.C.B.). The Affymetrix sample work was performed in the UCI DNA MicroArray Facility. The authors report no conflicts of interest. The authors alone are responsible for the content and writing of the paper.

References

Aguilar JS, Devi-Rao GV, Rice MK, Sunabe J, Ghazal P, Wagner EK (2006). Quantitative comparison of the HSV-1 and HSV-2 transcriptomes using DNA microarray analysis. *Virology* **348:** 233–241.

Aguilar JS, Ghazal P, Wagner EK (2005). Design of a herpes simplex virus type 2 long oligonucleotide-based microarray: global analysis of HSV-2 transcript abundance during productive infection. *Methods Mol Biol* **292:** 423–448.

Amici C, Belardo G, Rossi A, Santoro MG (2001). Activation of I kappa b kinase by herpes simplex virus type 1. A novel target for anti-herpetic therapy. *J Biol Chem* **276:** 28759–28766.

Banati RB (2003). Neuropathological imaging: in vivo detection of glial activation as a measure of disease and adaptive change in the brain. *Br Med Bull* **65:** 121–131.

Bloom DC, Lokensgard JR, Maidment NT, Feldman LT, Stevens JG (1994). Long-term expression of genes

in vivo using non-replicating HSV vectors. *Gene Therapy* **1(Suppl 1):** S36–S38.

Bowers WJ, Olschowka JA, Federoff HJ (2003). Immune responses to replication-defective HSV-1 type vectors within the CNS: implications for gene therapy. *Gene Therapy* **10:** 941–945.

Brukman A, Enquist LW (2006). Suppression of the interferon-mediated innate immune response by pseudorabies virus. *J Virol* **80:** 6345–6356.

Burton EA, Fink DJ, Glorioso JC (2002). Gene delivery using herpes simplex virus vectors. *DNA Cell Biol* **21:** 915–936.

Calvano SE, Xiao W, Richards DR, Felciano RM, Baker HV, Cho RJ, Chen RO, Brownstein BH, Cobb JP, Tschoeke SK, et al. (2005). A network-based analysis of systemic inflammation in humans. *Nature* **437:** 1032–1037.

Chirgwin JM, Przybyla AE, MacDonald RJ, Rutter WJ (1979). Isolation of biologically active ribonucleic acid from sources enriched in ribonuclease. *Biochemistry* **18:** 5294–5299.

DeLuca NA, McCarthy AM, Schaffer PA (1985). Isolation and characterization of deletion mutants of herpes simplex virus type 1 in the gene encoding immediate-early regulatory protein ICP4. *J Virol* **56:** 558–570.

Dobson AT, Margolis TP, Sedarati F, Stevens JG, Feldman LT (1990). A latent, nonpathogenic HSV-1-derived vector stably expresses beta-galactosidase in mouse neurons. *Neuron* **5:** 353–360.

Dumas T, McLaughlin J, Ho D, Meier T, Sapolsky R (1999). Delivery of herpes simplex virus amplicon-based vectors to the dentate gyrus does not alter hippocampal synaptic transmission in vivo. *Gene Therapy* **6:** 1679–1684.

Eidson KM, Hobbs WE, Manning BJ, Carlson P, DeLuca NA (2002). Expression of herpes simplex virus ICP0 inhibits the induction of interferon-stimulated genes by viral infection. *J Virol* **76:** 2180–2191.

Friedman HM, Wang L, Fishman NO, Lambris JD, Eisenberg RJ, Cohen GH, Lubinski J (1996). Immune evasion properties of herpes simplex virus type 1 glycoprotein gC. *J Virol* **70:** 4253–4260.

Goodkin ML, Morton ER, Blaho JA (2004). Herpes simplex virus infection and apoptosis. *Int Rev Immunol* **23:** 141–172.

Goodkin ML, Ting AT, Blaho JA (2003). NF-kappaB is required for apoptosis prevention during herpes simplex virus type 1 infection. *J Virol* **77:** 7261–7280.

Guillemin GJ, Brew BJ (2004). Microglia macrophages perivascular macrophages and pericytes: a review of function and identification. *J Leukoc Biol* **75:** 388–397.

Higaki S, Gebhardt BM, Lukiw WJ, Thompson HW, Hill JM (2002). Effect of immunosuppression on gene expression in the HSV-1 latently infected mouse trigeminal ganglion. *Investig Ophthalmol Vis Sci* **43:** 1862–1869.

Hill JM, Lukiw WJ, Gebhardt BM, Higaki S, Loutsch JM, Myles ME, Thompson HW, Kwon BS, Bazan NG, Kaufman HE (2001). Gene expression analyzed by microarrays in HSV-1 latent mouse trigeminal ganglion following heat stress. *Virus Genes* **23:** 273–280.

Ho DY, Fink SL, Lawrence MS, Meier TJ, Saydam TC, Dash R, Sapolsky RM (1995). Herpes simplex virus vector system: analysis of its in vivo and in vitro cytopathic effects. *J Neurosci Methods* **57:** 205–215.

Johnson PA, Miyanohara A, Levine F, Cahill T, Friedmann T (1992). Cytotoxicity of a replication-defective mutant of herpes simplex virus type 1. *J Virol* **66:** 2952–2965.

Johnson PA, Wang MJ, Friedmann T (1994). Improved cell survival by the reduction of immediate-early gene expression in replication-defective mutants of herpes simplex virus type 1 but not by mutation of the virion host shutoff function. *J Virol* **68:** 6347–6362.

Khodarev NN, Advani SJ, Gupta N, Roizman B, Weichselbaum RR (1999). Accumulation of specific RNAs encoding transcriptional factors and stress response proteins against a background of severe depletion of cellular RNAs in cells infected with herpes simplex virus 1. *Proc Natl Acad Sci U S A* **96:** 12062–12067.

Kramer MF, Cook WJ, Roth FP, Zhu J, Holman H, Knipe DM, Coen DM (2003). Latent herpes simplex virus infection of sensory neurons alters neuronal gene expression. *J Virol* **77:** 9533–9541.

Kurt-Jones EA, Chan M, Zhou S, Wang J, Reed G, Bronson R, Arnold MM, Knipe DM, Finberg RW (2004). Herpes simplex virus 1 interaction with Toll-like receptor 2 contributes to lethal encephalitis. *Proc Natl Acad Sci U S A* **101:** 1315–1320.

Li C, Wong WH (2001). Model-based analysis of oligonucleotide arrays: expression index computation and outlier detection. *Proc Natl Acad Sci U S A* **98:** 31–36.

Lin R, Noyce RS, Collins SE, Everett RD, Mossman KL (2004). The herpes simplex virus ICP0 RING finger domain inhibits IRF3- and IRF7-mediated activation of interferon-stimulated genes. *J Virol* **78:** 1675–1684.

Lowenstein PR (2002). Immunology of viral-vector-mediated gene transfer into the brain: an evolutionary and developmental perspective. *Trends Immunol* **23:** 23–30.

Marques CP, Hu S, Sheng W, Cheeran MC, Cox D, Lokensgard J.R (2004). Interleukin-10 attenuates production of HSV-induced inflammatory mediators by human microglia. *Glia* **47:** 358–366.

Marques CP, Hu S, Sheng W, Lokensgard JR (2006). Microglial cells initiate vigorous yet non-protective immune responses during HSV-1 brain infection. *Virus Res* **121:** 1–10.

Morrison LA (2004). The Toll of herpes simplex virus infection. *Trends Microbiol* **12:** 353–356.

Mossman K (2005). Analysis of anti-interferon properties of the herpes simplex virus type I ICP0 protein. *Methods Mol Med* **116:** 195–205.

Olschowka JA, Bowers WJ, Hurley SD, Mastrangelo MA, Federoff HJ (2003). Helper-free HSV-1 amplicons elicit a markedly less robust innate immune response in the CNS. *Mol Ther* **7:** 218–227.

Pasieka TJ, Baas T, Carter VS, Proll SC, Katze MG, Leib DA (2006). Functional genomic analysis of herpes simplex

virus type 1 counteraction of the host innate response. *J Virol* **80:** 7600–7612.

Paulus C, Sollars PJ, Pickard GE, Enquist LW (2006). Transcriptome signature of virulent and attenuated pseudorabies virus-infected rodent brain. *J Virol* **80:** 1773–1786.

Peden CS, Burger C, Muzyczka N, Mandel RJ (2004). Circulating anti-wild-type adeno-associated virus type 2 (AAV2) antibodies inhibit recombinant AAV2 (rAAV2)-mediated but not rAAV5-mediated, gene transfer in the brain. *J Virol* **78:** 6344–6359.

Peterson PK, Remington JS (2000). New concepts in the immunopathogenesis of CNS infections. Malden, MA: Blackwell Science.

Singh J, Wagner EK (1995). Herpes simplex virus recombination vectors designed to allow insertion of modified promoters into transcriptionally "neutral" segments of the viral genome. *Virus Genes* **10:** 127–136.

Stingley SW, Ramirez JJ, Aguilar SA, Simmen K, Sandri-Goldin RM, Ghazal P, Wagner EK (2000). Global analysis of herpes simplex virus type 1 transcription using an oligonucleotide-based DNA microarray. *J Virol* **74:** 9916–9927.

Sun A, Devi-Rao GV, Rice MK, Gary LW, Bloom DC, Sandri-Goldin RM, Ghazal P, Wagner EK (2004). Immediate-early expression of the herpes simplex virus type 1 ICP27 transcript is not critical for efficient replication in vitro or in vivo. *J Virol* **78:** 10470–10478.

Taddeo B, Esclatine A, Roizman B (2002). The patterns of accumulation of cellular RNAs in cells infected with a wild-type and a mutant herpes simplex virus 1 lacking the virion host shutoff gene. *Proc Natl Acad Sci U S A* **99:** 17031–17036.

Taddeo B, Luo TR, Zhang W, Roizman B (2003). Activation of NF-kappaB in cells productively infected with HSV-1 depends on activated protein kinase R and plays no apparent role in blocking apoptosis. *Proc Natl Acad Sci U S A* **100:** 12408–12413.

Taddeo B, Zhang W, Lakeman F, Roizman B (2004). Cells lacking NF-kappaB or in which NF-kappaB is not activated vary with respect to ability to sustain herpes simplex virus 1 replication and are not susceptible to apoptosis induced by a replication-incompetent mutant virus. *J Virol* **78:** 11615–11621.

Tsavachidou D, Podrzucki W, Seykora J, Berger SL (2001). Gene array analysis reveals changes in peripheral nervous system gene expression following stimuli that result in reactivation of latent herpes simplex virus type 1: induction of transcription factor Bcl-3. *J Virol* **75:** 9909–9917.

Wagner EK (2006). The development of microarrays for analyzing hsv gene expression. In Alpha herpesviruses: molecular and cellular biology. Sandri-Goldin RM (ed). Wymondham, UK: Caister Academic, pp 121–134.

Wagner EK, Bloom DC (1997). Experimental investigation of herpes simplex virus latency. *Clin Microbiol Rev* **10:** 419–443.

Wagner EK, Ramirez JJ, Stingley SW, Aguilar SA, Buehler L, Devi-Rao GB, Ghazal P (2002). Practical approaches to long oligonucleotide-based DNA microarray: lessons from herpesviruses. *Prog Nucleic Acid Res Mol Biol* **71:** 445–491.

Wood MJ, Byrnes AP, Kaplitt MG, Pfaff DW, Rabkin SD, Charlton HM (1994). Specific patterns of defective HSV-1 gene transfer in the adult central nervous system: implications for gene targeting. *Exp Neurol* **130:** 127–140.

Yang WC, Devi-Rao GV, Ghazal P, Wagner EK, Triezenberg SJ (2002). General and specific alterations in programming of global viral gene expression during infection by VP16 activation-deficient mutants of herpes simplex virus type 1. *J Virol* **76:** 12758–12774.

This paper was first published online on Early Online on 25 January 2010.